JOURNAL OF CATALYSIS 71, 9–20 (1981)

A Molecular-Beam Study of the Reactions of Na and CsCl on a Carbon-Covered Surface

LEIF HOLMLID AND JIM O. OLSSON

Department of Physical Chemistry, University of Göteborg and Chalmers University of Technology, S-412 96 Göteborg, Sweden

Received January 15, 1979; revised November 4, 1980

The surface-catalyzed reaction Na + CsCl → NaCl + $Cs^+ + e_F^-$ (where F indicates the Fermi level in the surface) has been studied on carbon-covered Pt (8% W) surfaces in a static experiment with two molecular beams with absolute measurements of the main flux densities. The reaction probability is close to unity at low temperature, and has been measured down to 10^{-4} at high temperature, where the reaction CsCl → Cs + Cl → $Cs^+ + e_F^-$ + Cl starts to dominate. A model combining both the direct exchange path Na + CsCl ⇄ NaCl + Cs and the dissociation–recombination path Na + CsCl ⇄ Na + Cs + Cl ⇄ NaCl + Cs is shown to give excellent agreement in some runs. Most reactive flux goes via the exchange path. In some runs strong departures from the model used exist, which are tentatively described as being due to the existence of two adsorbed states of Na on the surface. The state with lowest energy is considered to be less reactive. This is further supported by recent desorption measurements. The use of surface reactions N + CsCl → NCl + $Cs^+ + e_F^-$ in "reactive" surface ionization detectors for detecting general atomic beams N and measuring their absolute fluxes is discussed.

1. INTRODUCTION

In recent years several studies of reactions between gas molecules and surfaces with molecular-beam techniques have been performed. Nevertheless, the number of similar studies of reactions between adsorbed molecules on a surface is small. Most surface reactions of interest in the field of catalysis are of this type. In recent reviews (*1, 2*) some problems with the modulated beam phase-sensitive approach have been discussed. In the present work, a steady-state two-beam approach has been used to study a surface-catalyzed reaction, i.e., a reaction which proceeds with a negligible rate in the gas phase at the same temperature (e.g., in the beam intersection in front of the surface). By this method, large temperature and signal regions have been covered and information on the surface reactions has been found. As is well known from the theory of reactions in flow systems, the relevant rate parameters may be determined even in such a steady-state case, with no modulated fluxes. The method becomes even more informative if absolute values of the fluxes can be measured, as has been done in the experiments described here.

The surface reactive system reported on here is

$$\mathrm{Na} + \mathrm{CsCl} \rightarrow \mathrm{NaCl} + \mathrm{Cs} \rightarrow \mathrm{NaCl}_{(g)} + \mathrm{Cs}_{(g)}^{+} + e_F^{-}. \quad (1)$$

Index (g) means a gas-phase molecule, while F indicates the Fermi level in the surface. The surface, a Pt (8% W) surface, covered with a more or less graphitized carbon layer, is unchanged by the reaction and all products and reactants desorb. In the gas phase, the first step is endothermic by about 0.3 eV, and the second step (then leading to a free electron) is also endothermic by 3.87 eV. The desorption steps are endothermic, for Cs^+ probably around 1.9 eV and for NaCl of the order of 0.6 eV, as found for CsCl in this study. The barrier in the exchange step on the surface is probably negligible, and the overall surface reac-

0021-9517/81/090009-12$02.00/0

tion is very efficient. Thus, it is clearly surface catalyzed in the conventional meaning of this expression. On a metal surface, for example, the CsCl molecules dissociate and Cs, Cs^+, and probably also Cl desorb quite rapidly.

A preliminary study of an analogous system, $K + RbCl \rightarrow Rb^+ + e_F^- + KCl$ has been reported recently (*3, 4*). A short study of $Na + RbCl \rightarrow Rb^+ + e_F^- + NaCl$ has also been performed (unpublished). A few related reactive systems have been studied previously in other laboratories. The reaction $Ba + LiF \rightarrow BaF^+_{(g)} + e_F^- + Li$ on W has been studied in a static molecular-beam experiment (*5, 6*). The "suppression effect" reported in Ref. (*7*) is a lowering of, e.g., K^+ emission from a KI melt on a Pt surface when RbI is added. This effect was interpreted as due to $KI \rightarrow K^+ + I_{(g)} + e_F^-$ followed by $K^+ + RbI \rightarrow KI + Rb^+_{(g)}$.

Reactions of the type in Eq. (1) are of interest for several reasons. The original reason for continued studies was the possibility of identification and removal of disturbing experimental effects in crossed-beam reactive scattering experiments with "differential" surface ionization detection (*3, 4, 8*). It was also found that it should be possible to use reactions similar to Eq. (1) for detection of molecular beams by "reactive" surface ionization and for other analytical purposes, e.g., in gas chromatography. An atom N, for example, H, Li, Ca, or Al, which is difficult to ionize with ordinary surface ionization, may be converted by CsCl to yield Cs^+ ions and thereby measured. It is also of great interest to analyze different types of surface-catalyzed reactions in detail, to determine which are the fundamental reaction steps on the surface, and where the reactive interaction takes place. From such knowledge, it should be possible to improve existing catalytic systems. Especially since carbon is a widely used catalyst support, which may interact with the catalyst (spillover effects), the system studied in this work appears very interesting.

Preliminary experiments showed several interesting features.

1. Large reactive signals were obtained without any interfering noise or background in a straightforward steady-state experiment.

2. Surface reactions in cases like Eq. (1) give a reaction probability very close to unity under suitable conditions. By a comparison with Ref. (*1*), this feature is judged to be unique so far. The smallest reaction probability detected in the case studied here was 10^{-4}. Thus, the range over which the reaction is followed is large. The maximum temperature dependence of the signal, corresponding to a slope of 6.8 eV, was remarkably large.

3. Absolute flux densities of the reactant molecular beams can be measured by surface ionization (for recent results, see Refs. (*9, 10*). Thus, absolute surface densities can be found from desorption measurements, giving absolute values of preexponential factors in bimolecular surface reactions. Such values appear to be rare (*1*).

4. A direct three-atom exchange reaction on the surface appeared consistent with the data. Since dissociation of CsCl on carbon-covered surfaces is small but nevertheless interferes with the reactive measurements, a dissociative (dissociation–recombination) reactive mechanism could compete. A study to distinguish between the two possibilities appeared very interesting from a fundamental point of view.

2. REACTION MODEL

In a reaction of the type considered here, Eq. (1), at least two different reaction paths appear possible. One, which is similar to the gas-phase reaction (*8, 11*), is the direct exchange reaction

$$Na + CsCl \rightleftarrows (Na\ Cl\ Cs) \rightleftarrows NaCl + Cs. \quad (2)$$

The other possible path is via a dissociation–recombination step of the alkali halide

TABLE 1

Reactions Included in the Combined Model with the Net Formula Na + CsCl → NaCl + Cs^+ + e_F^-

Adsorption–desorption	Dissociation–recombination	Exchange reaction
$CsCl_{(s)} \underset{f_{CsCl}}{\overset{k_{CsCl}}{\rightleftharpoons}} CsCl_{(g)}$		
$Cs_{(s)} \underset{f_{Cs}}{\overset{k_{Cs}}{\rightleftharpoons}} Cs_{(g)}$	$CsCl_{(s)} \underset{k_{r1}}{\overset{k_{d1}}{\rightleftarrows}} Cs_{(s)} + Cl_{(s)}$	
$Cs_{(s)} \xrightarrow{k_{Cs^+}} Cs_{(g)}^+ + e_F^-$		
$Cl_{(s)} \underset{f_{Cl}}{\overset{k_{Cl}}{\rightleftarrows}} Cl_{(g)}$		$CsCl_{(s)} + Na_{(s)} \underset{k_{e2}}{\overset{k_{e1}}{\rightleftarrows}} Cs_{(s)} + NaCl_{(s)}$
$Na_{(s)} \underset{f_{Na}}{\overset{k_{Na}}{\rightleftarrows}} Na_{(g)}$	$NaCl_{(s)} \underset{k_{r2}}{\overset{k_{d2}}{\rightleftarrows}} Na_{(s)} + Cl_{(s)}$	
$Na_{(s)} \xrightarrow{k_{Na^+}} Na_{(g)}^+ + e_F^-$		
$NaCl_{(s)} \xrightarrow{k_{NaCl}} NaCl_{(g)}$		

Note. The symbols f_i indicate fluxes to the surface, while k_i are rate constants on the surface.

$$\text{Na} + \text{CsCl} \rightleftarrows \text{Na} + \text{Cs} + \text{Cl} \rightleftarrows \text{NaCl} + \text{Cs}. \quad (3)$$

Since the Cs^+ signal from dissociation of CsCl is comparable in size to the signal from reaction in the middle-temperature range (see below), the dissociation must be included in the analysis. Since the species Cl and NaCl will compete for the Cs atoms, an interaction between the two reaction paths is possible. Thus, both Eqs. (2) and (3) must be considered simultaneously.

In Table 1, all the reactions and desorption channels considered are displayed. Since it has been found that alkali halide beams from thermal sources contain a dissociated fraction, consisting of alkali and probably also of halogen atoms (*3, 12, 13*), fluxes of Cs and Cl are included. The energy levels associated with all the reaction steps are shown in Fig. 1.

3. EXPERIMENTAL

The apparatus was almost identical to the one in Ref. (*10*). The Na oven was a simple two-chamber effusive oven, with a back temperature of 540–590 K. The front temperature was kept 40–60 K higher. The CsCl oven was mounted close to the studied surface and was also of a two-chamber design, with back temperatures of 740–840 K and front temperatures 30–50 K higher. The emitting surface was a circular many-channel array with a diameter of 3 mm (collimated hole structure with pore diameter 50 μm and length 3 mm; delivered by Brunswick Corporation, Chicago, Ill.). The oven was mounted at an angle of about 25° to the alkali beam. The CsCl was of high purity (Kawecki-Berylco Industries, Inc.) containing Rb (800 ppm), K (15 ppm), and Na (100 ppm) as the main impurities. Each oven had a beam flag. For dimensions and further details, see Fig. 2.

The Pt (8% W) (here called PtW) surface was in ribbon form, 14 × 0.7 × 0.025 mm^3

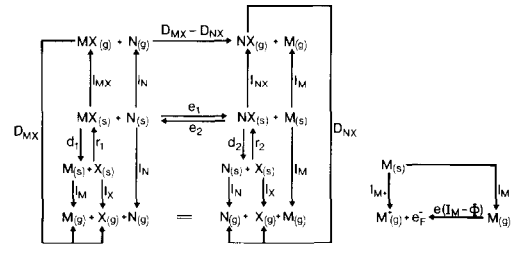

FIG. 1. Energy diagram giving the various energy cycles used in the reaction model N + MX → NX + M^+ + e_F^-. Both the dissociation–recombination reactions and the exchange reactions on the surface may contain activation barriers.

(obtained from Sigmund Cohn Company, Mount Vernon, N.Y. as alloy No. 479). The ribbon was dc heated and held at 60–90 V with respect to ground. The surrounding ion collector was connected to an electrometer at ground potential. In the collector, openings were made to allow the beams to reach one side of the ribbon, as shown in Fig. 2. The CsCl beam flux covered a 6-mm height of the ribbon, while the central 4-mm part was also covered by the Na beam. Three different ribbons have been used in the six experimental runs in this paper, the first in runs 1 and 3, the second in run 2, and the third in runs 4–6. A beam flag could intercept either of the two beams or both.

The ribbon temperature was determined in the same way as in Ref. (*9*). Thus, nonpyrometric temperatures in the range 1150–830 K were calculated from the heating currents.

Before and after each experimental run, the surface was treated with oxygen, admitted through a leak valve and a tube with its end inside the cooled shield, at a pressure of 10^{-4} Torr for 10–100 min in the detector chamber (1 Torr = 133 Pa). The temperature of the surface was 1000–1100 K, which is suitable for removal of carbon from the surface (*14, 15*). This gave an electron emission corresponding to an effective work function of 6 V. According to Wilf and Dawson (*16*), this treatment may give a

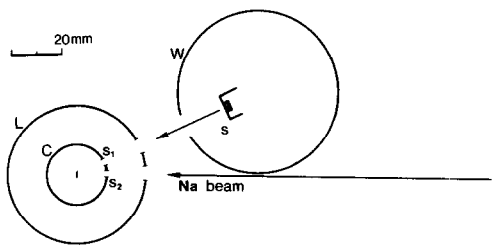

FIG. 2. Cut through apparatus, top view. The distance between the Na source and the surface is 440 mm. The slits S_1 and S_2 have the dimensions 6 × 3.5 and 4 × 2.5 mm², with the height given first. W: water-cooled shield around CsCl oven. S: CsCl source. L: liquid nitrogen-cooled shield around surface. C: collector for desorbing ions around the surface.

quite stable oxide layer on the surface. After that the constancy of the beam fluxes was checked and their absolute values were measured during continuous oxygen inlet at 5×10^{-6} Torr. That the ionization coefficients β for Na and CsCl on the oxygenated surface were very close to unity was verified by the observed independence of the ion current on the heating current. The beam attenuation due to gas scattering was eliminated by turning the oxygen inlet off rapidly and taking the reading at the highest signal value, at 1–5% above the value with gas on.

The surface was carbon (graphite) covered (*9, 17*) at a butane (uncorrected) pressure reading of 1×10^{-5} Torr at 1750 K, which gave an electron effective work function of 4.47–4.60 V at 1500 K. Due to the disappearance of all metal peaks during such a treatment in Auger electron spectroscopy measurements (*18*), it is believed that at least a few layers of carbon cover the surface. The ion signal was then measured, at a background pressure of 1×10^{-6} Torr, as a function of temperature, starting at high temperature for three different settings of the beam flags, viz., (1) only the CsCl beam on, (2) only the Na beam on, and (3) both beams on. The results are shown in Figs. 3 and 4 for two different runs. Checks of work function and beam flux constancy were made between the three sets of measurements. The effective work function from the surface ionization of Na and the total Na flux, in case (2) above, was found to be 4.54–4.61 V, not using the very low temperature region. The background current with the beam flux turned off was measured in connection with the signal current, and subsequently subtracted. Due to diffusion into the surface layer of the beam substances, great care had to be taken to measure the true steady-state values accurately, especially in the regions with slow signal response. Temporary temperature decreases to increase the rate of diffusion into the surface or removal of the diffused densities at higher tempera-

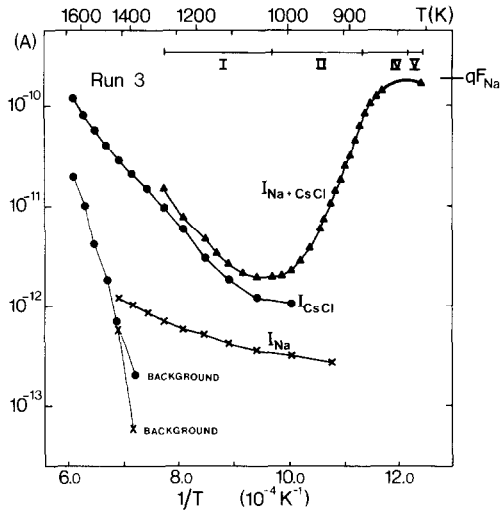

FIG. 3. Experimental results with each beam on and with both beams on, $I_{Na+CsCl}$, for run 3. The continuous curve in regions IV and V replaces closely spaced measurement points.

ture were thus employed to reach the desired steady-state conditions.

The two-beam method used in the experiments allows the reaction region to be well defined. In this case, the CsCl beam covers a slightly larger part of the ribbon than the Na beam (6-mm height versus 4 mm). The entire Na flux may interact with the CsCl on the surface. Thus, qF_{Na} may be directly compared with the reactive signal ΔI, which is necessary to obtain valid information on the usefulness of a "chemical" surface ionization molecular-beam detector. Since F_{CsCl} is much larger than F_{Na}, the CsCl surface density is almost unchanged by the reaction and is practically the same in the two regions of the surface, with and without Na flux. Thus the possible long-range migration of Na atoms and CsCl molecules over the surface will not influence the results (cf. Ref. (*2*)).

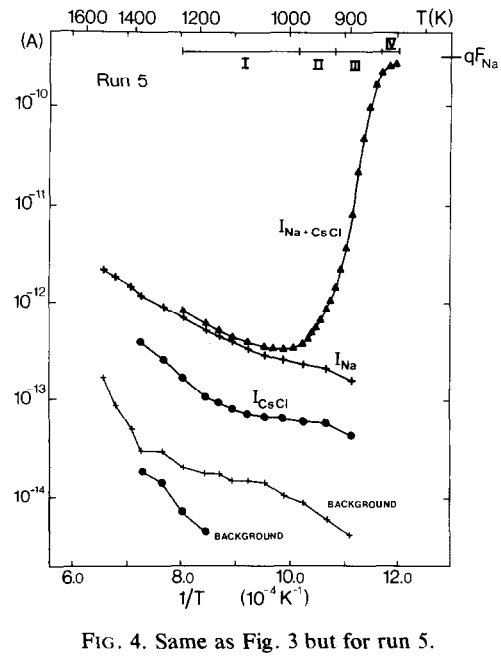

FIG. 4. Same as Fig. 3 but for run 5.

4. RESULTS

The quantity

$$\Delta I = I_{Na+CsCl} - I_{Na} - I_{CsCl}, \qquad (4)$$

approximately equal to the true reactive current, has been plotted in Fig. 5. To relate all fluxes and currents to the same area, the measured values of I_{CsCl} have been reduced by a factor of $\frac{2}{3}$. The similarity of all the curves is striking, and the subdivision of the curves in several rather well-defined regions, I–V as in Figs. 3 and 4, is

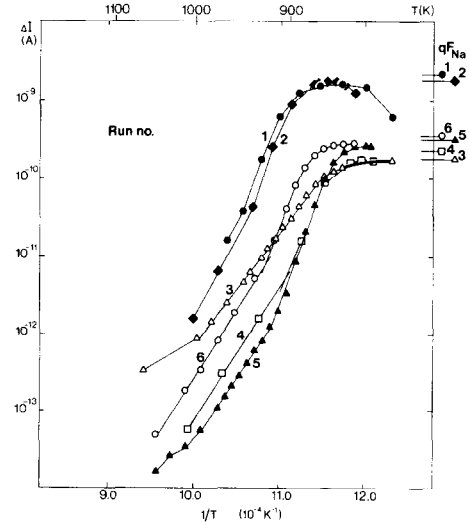

FIG. 5. $\Delta I = I_{Na+CsCl} - I_{Na} - I_{CsCl}$, for the six runs. ΔI is an approximate measure of the amount of reaction. To the right, the Na beam fluxes in current units, qF_{Na}, are plotted. The heavy continuous curve for run 3 replaces closely spaced measurement points.

TABLE 2

Reaction Parameters γ_i Defined in Terms of Rate Constants from Table 1 and in Terms of Final Fit Parameters ϵ_i and l_i

$\gamma_1 = (k_{Cs} + k_{Cs^+})k_{Cl}/k_{r1}$	$= \epsilon_1 \exp[(e(\Phi - I_{Cs}) - D_{CsCl} - l_1)/kT]$
$\gamma_2 = (k_{Na} + k_{Na^+})k_{Cl}/k_{r2}$	$= \epsilon_2 \exp[(-D_{NaCl} - l_2)/kT]$
$\gamma_3 = \gamma_1 k_{d1}/k_{CsCl}$	$= \epsilon_1\epsilon_3 \exp[(e(\Phi - I_{Cs}) - D_{CsCl})/kT]$
$\gamma_4 = \gamma_2 k_{d2}/k_{NaCl}$	$= \epsilon_2\epsilon_4 \exp[-D_{NaCl}/kT]$
$\gamma_5 = (k_{Na} + k_{Na^+})k_{CsCl}/k_{e1}$	$= \epsilon_5 \exp[-l_5/kT]$
$\gamma_6 = (k_{Cs} + k_{Cs^+})k_{NaCl}/k_{e2}$	$= \epsilon_6 \exp[(-l_5 - D_{CsCl} + D_{NaCl} + e(\Phi - I_{Cs}))/kT]$
$l_1 = l_{CsCl} - d_1$	$\beta = \alpha/(1 + \alpha)$
$l_2 = l_{NaCl} - d_2$	$\alpha = \frac{1}{2} \exp[e(\Phi - I)/kT]$
$l_5 = l_{CsCl} + l_{Na} - e_1$	

Note. All parameters γ_i have the dimension $m^{-2} s^{-1}$. α and β are the degree of surface ionization and ionization coefficient.

easily made. However, note that run 3 and possibly also run 1 show only one slope in the plots, while the other runs show two distinctly different slopes.

A steady-state solution of the rate equations describing the set of reactions in Table 1 gives the Cs^+ flux density leaving the surface as a function of several parameters, given in Table 2 (*19*). The fourth-order equation in i_{Cs^+} has been solved using the subroutine ZANLYT from the IMSL library. For a full comparison with experimental data,

$$I = I_{Na+CsCl} - I_{Na} \qquad (5)$$

has been used. The comparison between theory and the experimental data uses only the two runs 3 and 5, since most data exist for these two runs and since they are extremes regarding the beam intensity ratio F_{Na}/F_{CsCl} (Table 3). No further information seems to exist in the other runs. Both I_{CsCl} and I, Eq. (5), have been used to find the parameter values. The best-fit parameter values are collected in Table 4, while the fits are shown in Figs. 6–8.

The flux densities required are found from the absolute fluxes measured, using the reaction area Y in Table 4. F_{CsCl} and F_{Na} are known, while F_{Cs} and F_{Cl} are more difficult to deduce directly from the experiments. This point will be discussed elsewhere (*12*).

All dimers in the beams are assumed to dissociate on the surface. All beam particles, possibly excluding Cl, are likely to stick to the surface with an accommodation coefficient close to unity.

The three dissociation parameters l_1, ϵ_1, and ϵ_3 have been found from three-parameter fits to I_{CsCl}, which usually has been measured to higher temperatures than I.

TABLE 3

Experimental Quantities for the Six Absolute Runs

Run no.	qF_{CsCl} (A)	qF_{Na} (A)	ΔI_{max} (A)	$1 - \Delta I_{max}/qF_{Na}$	$q^2F_{CsCl} \times F_{Na}$ (A^2)	F_{Na}/F_{CsCl}
1	8.7×10^{-8}	2.3×10^{-9}	1.73×10^{-9}	0.25	2.0×10^{-16}	2.6×10^{-2}
2	1.6×10^{-7}	1.96×10^{-9}	1.89×10^{-9}	0.04	3.1×10^{-16}	1.2×10^{-2}
3	2.3×10^{-7}	1.90×10^{-10}	1.85×10^{-10}	0.03	4.4×10^{-17}	8.3×10^{-4}
4	6.7×10^{-8}	2.2×10^{-10}	1.89×10^{-10}	0.14	1.5×10^{-17}	3.3×10^{-3}
5	1.5×10^{-8}	3.3×10^{-10}	2.82×10^{-10}	0.17	5.1×10^{-18}	2.3×10^{-2}
6	1.15×10^{-7}	3.7×10^{-10}	3.00×10^{-10}	0.19	4.3×10^{-17}	3.2×10^{-3}

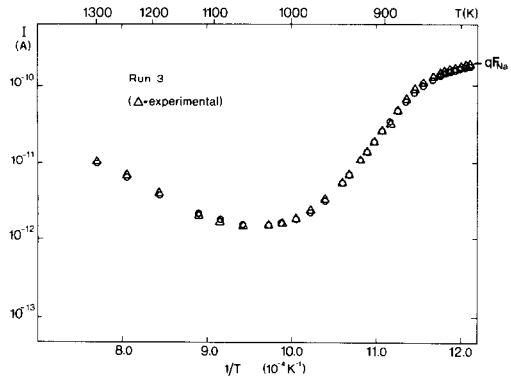

FIG. 6. Best fit to run 3, with parameter values given in Table 4.

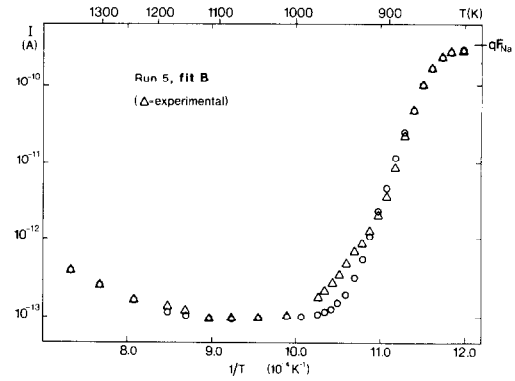

FIG. 8. Same as Fig. 7, but for fit B.

Further data will be given in a forthcoming article (*12*). In the fits to I, these three parameters are only changed slightly to improve the fits in region I, as shown in Table 4. This is easily possible, since they do not influence the results in the other regions. Parameters ϵ_4 and ϵ_6 do not influence the fits and have been put equal to ϵ_3 and ϵ_5, respectively. ϵ_6 is important in run 5, fit B. Further, ϵ_2 and l_2 interact strongly. *Thus, effectively only three parameters remain to fit the reactive data in regions II–IV, namely* ϵ_5, l_5, *and* ϵ_2 (*or* l_2). As may be seen from the fits to run 5, *the remaining functional form cannot describe all experimental results*, even if the beam fluxes also are varied in the final stages. The three available parameters influence the computed curves very differently (Fig. 9), and they are thus reliably determined in the procedure.

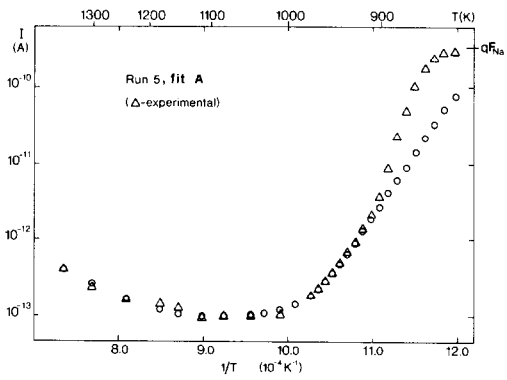

FIG. 7. Best fit to run 5, fit A. The set of parameter values is given in Table 4.

In run 5, which has the shape with two slopes (regions II and III), no possibility has been found to fit the data even with the combined model in Table 1. However, by the use of two different sets of ϵ_5, ϵ_6, and l_5, one set for regions I and II (run 5, fit A), and the second set for regions I, III, and IV (run 5, fit B), a good fit of the results has been found. Observe that most of the other parameters change only slightly between runs 3 and 5. Such a constancy in the parameters exists also for other runs.

The low-temperature plateau, region IV, is 3–25% lower than qF_{Na} for all runs (see Table 3). This is easily reproduced by decreasing ϵ_6 so that $\gamma_6 \leq \gamma_5$ (cf. Fig. 9).

If the parameter γ_1 is very small and γ_2 very large (see Table 2), the limiting case with only exchange reaction is reached. In regions II–IV, a quite good fit is still found, which means that most product is formed by the exchange reaction. If instead the parameters γ_5 and γ_6 are increased strongly, the exchange reaction path disappears. In this case the product signal below region I increases very slowly with decreasing temperature, and no large reaction probability is found. Thus, the exchange reaction is the dominating path.

The solution of the complete reaction set (Table 2) for i_{Cs^+} has been checked by comparison with the corresponding solu-

TABLE 4

Values of Constants, Fluxes, and Parameters used in the Fits in Figs. 6–8

	Run 3	Run 5, fit A	Run 5, fit B
qF_{CsCl} (A)	2.33×10^{-7}	1.53×10^{-8}	
qF_{Na} (A)	1.90×10^{-10}	3.30×10^{-10}	
qF_{Cs} (A)	4.8×10^{-12}	5.8×10^{-13}	
qF_{Cl} (A)	4.0×10^{-12}	5.4×10^{-13}	
l_1 (eV)	-1.30 [-1.30]	-1.30	
l_2 (eV)	-1.15[a]	-1.30[a]	
l_5 (eV)	3.45	3.45	6.80
ϵ_1 (m^{-2} s^{-1})	9.0×10^{23} [9.0×10^{23}]	4.0×10^{21}	
ϵ_2 (m^{-2} s^{-1})	1.2×10^{29} [a]	3.8×10^{27} [a]	
ϵ_3	4.3 [4.3]	1.0	
ϵ_4	(4.3)	(4.3)	
ϵ_5 (m^{-2} s^{-1})	5.0×10^{37}	7.5×10^{37}	2.0×10^{56}
ϵ_6 (m^{-2} s^{-1})	(5.0×10^{37})	(7.5×10^{37})	8.0×10^{53}

Note. The values in parentheses do not influence the fits very much. Values in brackets are from three-parameter fits to I_{CsCl} (*12*). Constants: $\Phi_{PtW} = 4.55$ V; $I_{Cs} = 3.87$ V; $D_{CsCl} = 4.61$ eV; $D_{NaCl} = 4.23$ eV; $Y = 2.8 \times 10^{-6}$ m^2.

[a] Interaction between l_2 and ϵ_2. Smaller $|l_2|$ gives larger ϵ_2.

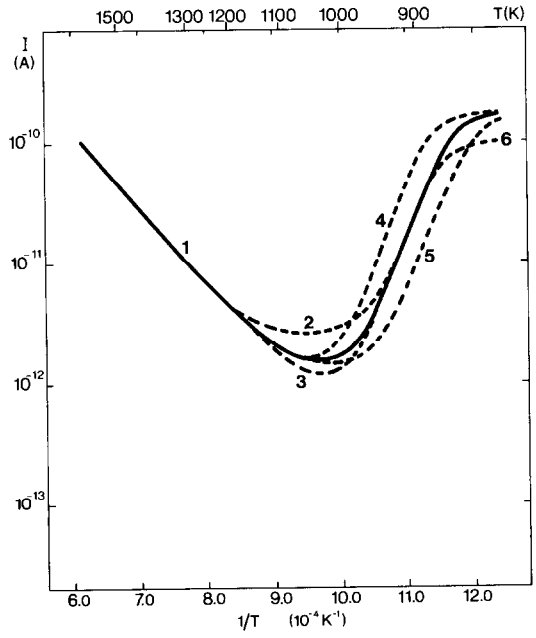

FIG. 9. Changes in some parameters for run 3. Curve 1: best fit, values in Table 4. Curve 2: $\epsilon_2 = 1.2 \times 10^{28}$ m^{-2} s^{-1}. Curve 3: $\epsilon_2 = 1.2 \times 10^{30}$ m^{-2} s^{-1}. Curve 4: $l_5 = 3.55$ eV. Curve 5: $l_5 = 3.35$ eV. Curve 6: $\epsilon_6 = 5.0 \times 10^{32}$ m^{-2} s^{-1}. Other parameters are as in curve 1. The effect of changes in l_2 and ϵ_2 is very similar.

tion of the case with no exchange reaction. In that case a third-degree equation for i_{Cs^+} is valid. The agreement at high temperature is good. Furthermore, the solution in the case with only the exchange reaction agrees well with the combined reaction case in the low-temperature region.

5. DISCUSSION

5.1. Some Experimental Characteristics

1. The low-temperature plateau, region IV, corresponds to almost-complete conversion of Na to desorbing Cs^+. That the reaction probability is slightly smaller than unity may have at least three causes (besides unnoticed drifts, etc.): (a) the existence of the reverse exchange reaction Cs + NaCl, which can be taken into account to improve the fits in region IV, as noted above, (b) the flux of Cl, which exists in the CsCl beam, and (c) a decrease in the work function due to Na coverage, such that β_{Cs} decreases. None of the three possible causes can be rejected, even though possibility (a) appears most important.

2. The strong temperature variation of the signal in region II depends on the large

value of $l_5 = l_{CsCl} + l_{Na} - e_1$, i.e., on the fact that the sum of the desorption energies of the reactants is much larger than the activation barrier for the surface exchange reaction. In the case of K + RbCl (*3, 4*), $l_5 \approx 3.8$ eV was found, which is close to 3.45 eV found here.

3. The dependence of the signal in region II on the beam fluxes in Figs. 5 and 10 indicates first-order reactions for Na and CsCl. The variation in product flux is almost two orders of magnitude. It is apparent that the surface coverage is very small at the temperature used for Fig. 10.

4. The low-temperature signal drop in region V is due to increased surface coverage, mainly by Na, in this region. The coverage probably does not approach one monolayer until the signal drops down very far. A change $e\Delta\Phi = 0.68$ eV in the system Na on Ni (*20*) was reported for $0.05 < \theta < 0.15$ of a monolayer. Such a large change in work function is found only at the lowest-temperature point of I in run 1 in Fig. 5.

5. The rise of the Cs^+ signal in region I is due to increased dissociation of CsCl on the surface. This is seen directly in Figs. 3 and 4 and is confirmed by the fits of the model with $F_{Na} = 0$ to the data I_{CsCl} (Table 4). Further details will be given in Ref. (*12*).

6. Virtually no reaction Na + CsCl → Cs + NaCl takes place in the beam intersection in front of the surface. Such a reaction should give a temperature-independent current of Cs^+ from the surface, which if it exists must be $\leq 10^{-4} \times F_{Na}$ as seen in Fig. 5. Thus, the reaction could be said to be surface catalyzed.

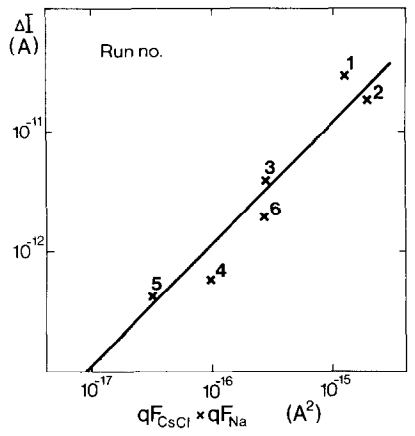

FIG. 10. Product signal ΔI at 950 K, as a function of the product of beam fluxes. The line is not fitted but drawn to give a linear relationship, $I \propto F_{CsCl} \times F_{Na}$.

5.2. *Region III*

In Fig. 5 a few systematic variations can be identified concerning the approximately 6.8-eV slope in region III in all runs except run 3:

1. The correlation between F_{Na}/F_{CsCl} and the size of region III, such that a low value of this quantity is found in cases with small region III.

2. The variation of the location of the apparent break point between regions II and III in Fig. 5 with Na beam flux. For a small flux the break point moves to a lower temperature. Thus, the product flux in region III does not depend linearly on $F_{Na} \times F_{CsCl}$.

3. The variation of the temperature at the maximum in the curves with Na beam flux. This means that the different curves cross each other in regions III and IV.

4. Further, a slow approach to steady state of $I_{Na+CsCl}$ has sometimes been observed in region II.

A direct interpretation of the very large values of l_5, ϵ_5, and ϵ_6 in fit B, run 5 (Table 4), in terms of the model used successfully for run 3 is not possible. This is due to the resulting large values of l_{CsCl}, l_{Na}, A_{CsCl}, and A_{Na}, which are believed to be nonphysical. The possibilities studied to explain this odd behaviour include surface changes, work function changes due to surface coverage, island formation of Na, and other reaction paths like Cl + Cl → Cl_2 or CsCl + Cl → Cs + Cl_2. However, none of these agrees well with the experiments.

In recent work on alkali desorption from carbon-covered platinum in our laboratory, several new features have been identified. The desorption process appears to be very complex. Some information has been pub-

lished (*21*), but several puzzles remain. Thus a detailed interpretation of region III is not yet possible, but the following dynamic picture is consistent with the experimental results.

It may be assumed that the Na atoms have at least two possible adsorbed states on the surface, one recessed (localized) or otherwise less reactive, and another migrating, with a smaller desorption energy (*22*). At low coverage an equilibrium distribution exists, but with increasing coverage at low temperature the nonreactive state becomes filled and the migratory-state population increases more rapidly than could result from the desorption rate changes. Thus, the reaction rate Na + CsCl increases rapidly towards lower temperature.

This mechanism is consistent with the Na flux correlations in 1, 2, and 3 above. In the case of point 3, the CsCl density plays a minor role, since the signal increases with decreasing temperature up to $\Delta I \approx qF_{Na}$ just before the signal starts to drop down due to Na surface coverage.

The postulated less reactive state of Na may be at grain boundaries, or may be at the centre of the carbon rings. The desorption from these locations is characterized by a large preexponential factor and desorption energy due to the large number of bonds to the surface involved (*22, 23*). This has been experimentally verified (*21, 24*) at low surface density.

The slow approach to equilibrium in region II may be tentatively explained as follows. The diffusion to and from the interior of the graphite may go via the localized state. At low coverage, equilibrium with the Na atom density inside the surface must be reached before the reactive signal stabilizes, while at high coverage the regions below the entrance points in the surface are already saturated and no slow process is observed.

5.3. Values of Surface Rate Parameters

If the relevant desorption rate parameters were known, surface reaction rate parameters could be determined from the best-fit values γ_i and l_i in Table 4. Due to the complicated and still incompletely understood desorption processes from the carbon surface (*3, 12, 21*), only a preliminary discussion is possible here. Work on these problems is in progress in our laboratory, and refined treatments will be possible later.

The dominant parameters describing the reaction are ϵ_5 and l_5. The value $\epsilon_5 = 5 \times 10^{37}$–$8 \times 10^{37}$ m^{-2} s^{-1} gives A_{e1}, the preexponential for the reaction Na + CsCl → Cs + NaCl, approximately equal to 2×10^{-7} m^2 s^{-1}, if $A_{CsCl} \approx 10^{13}$ s^{-1} and $A_{Na} \approx 10^{18}$ s^{-1} are assumed. The last value is the measured preexponential value for alkali atom desorption at low coverage (*21*) which may be too large to apply here. The value used for A_{CsCl} is the normal value for a migratory adsorption state. The resulting value for A_{e1} is only slightly smaller than the maximum collision theory value for bimolecular reactions on a surface, viz., $\approx 5 \times 10^{-7}$ m^2 s^{-1}. If A_{Na} is slightly smaller than 10^{18} s^{-1}, the value found for A_{e1} will also decrease, which probably is more realistic.

The value of $l_5 = 3.45$ eV gives $l_{CsCl} - e_1 = 0.55$ eV if a reasonable value of 2.9 eV is used for l_{Na}. This value for l_{Na} is slightly larger than the one found on many metal surfaces (*10*), 2.7 eV. It may be assumed that e_1 is small as in the corresponding gas-phase reaction (*25*), and thus that $l_{CsCl} \approx 0.6$ eV is valid. Combining this with the value of $l_1 = -1.30$ eV gives $d_1 \approx 1.9$ eV on the surface. This is considerably smaller than the gas-phase value 4.61 eV for CsCl (*26*).

The value for $l_{CsCl} = 0.6$ eV found here is lower than the heat of sublimation, 2.0 eV, and the dissociation energy for the dimer Cs_2Cl_2, equal to 1.6 eV (*26, 27*). The values of l_1 found for CsCl on Ir (111) covered by single-layer carbon by Zandberg *et al.* (*28*), −1.05 eV, and on graphite by Zandberg and Paleev (*29*), −(0.8–1.0) eV, are probably too small in an absolute sense since the recombination reaction and the atom flux in the beam have not been included in the

analysis, as will be further discussed in Ref. (*12*).

The values of ϵ_3 and ϵ_4 are expected from transition-state theory (*30*) to be somewhat larger than unity, which agrees with the values in Table 4. They have usually been put equal to unity in interpretations of experiments (*28, 29*).

The values of ϵ_1 and ϵ_2 found in the fits are more difficult to interpret. It should be noted that ϵ_1 is found from the high-temperature part and only describes the amount of dissociation. Thus, its value is not dependent on the choice of reaction model.

Rate parameters for the surface reactions derived from the fits are thus in agreement with general theoretical expectations. Unfortunately, there are as yet no directly measured experimental values for comparison. It is expected that such values will be generated in kinetic experiments in progress in our laboratory.

6. CONCLUSIONS

In a steady-state surface reaction experiment of the type described here, it is possible to distinguish between different reaction paths on the surface. In this case, the direct exchange reaction Na + CsCl $\rightarrow$ NaCl + $Cs^+ + e_F^-$ is shown to dominate over a reaction path proceeding via dissociation–recombination steps CsCl $\rightleftarrows$ Cs + Cl and Na + Cl $\rightleftarrows$ NaCl to the same end result. Such a distinction is usually difficult to reach even in modulated beam experiments, where direct kinetic information is available. By combination of kinetic desorption parameters and the absolute values of the parameters from the steady-state experiment, rate parameters for the surface reactions will be obtained. Due to the complicated desorption processes on the carbon-covered surface, this is, however, not yet possible. Desorption experiments with various techniques are in progress in our laboratory.

The very strong temperature dependence at low surface temperature in several of the experimental curves indicates a complication of the simple exchange reaction at large Na surface densities. A tentative model assumes filling of a localized Na adsorption state with increasing coverage and a simultaneously increasing occupation of a migrating state.

A dissociated fraction of 2×10^{-5} of the CsCl beam complicates the interpretation of the experiments. This type of nonequilibrium dissociation has been reported previously by one of us (*3*), and will be further discussed elsewhere (*12*).

The approach of the reaction probability to a value close to unity at low temperature shows that a "reactive" absolute surface ionization molecular-beam detector is feasible. Such a detector would retain the good selectivity of the ordinary surface ionization detector while broadening the range of atoms detected and measured absolutely.

APPENDIX: EQUILIBRIUM CONSIDERATIONS

The possibility of near equilibrium in some reactions on the surface is of interest. One possible reaction is Na + CsCl $\rightleftarrows$ Cs + NaCl. The requirement of equilibrium is that the flux in all other steps involving Na, CsCl, Cs, and NaCl should be much smaller than the flux in both directions of the exchange reaction. At 800 K in run 3, γ_5 is equal to 4×10^{-9} A which is much larger than i_{Na}. Thus, from Table 2, $k_{CsCl} \gg k_{e1} n_{Na}$ is valid and no equilibrium exists even in this case of unit reaction probability for Na. In the case of the reactions Cs + Cl $\rightleftarrows$ CsCl with $F_{Na} = 0$, equilibrium could exist. However, the desorption of CsCl is much too rapid to maintain equilibrium, which is found from $\gamma_3/\gamma_1 = k_{d1}/k_{CsCl}$ in Table 2. In run 3, this is equal to 3×10^{-8} at 800 K and 3×10^{-4} at 1600 K.

ACKNOWLEDGMENTS

We would like to thank fil.kand. Ewa Thylander, who took part in some preliminary experiments and in the design of the small halide oven. Fil.kand. Esa Rytööja took part in some of the final runs. This work was supported by the Swedish Natural Science Research Council.

REFERENCES

1. Somorjai, G. A., *J. Colloid Interface Sci.* **58,** 150 (1977).
2. Olander, D. R., *J. Colloid Interface Sci.* **58,** 169 (1977).
3. Holmlid, L., Dissertation, University of Göteborg, 1973.
4. Holmlid, L., *J. Chem. Phys.* **61,** 1244 (1974).
5. Ionov, N. I., and Mitsev, M. A., *Dokl. Akad. Nauk SSSR* **152** 137 (1963); Mitsev, M. A., *Sov. Phys. Tech. Phys.* **10,** 1621 (1966); see also Ref. (6).
6. Zandberg, É. Ya., and Ionov, N. I., "Surface Ionization." Israel Program for Scientific Translations, Jerusalem, 1971. [Transl. from Russian]
7. Kawano, H., and Inouye, H., *J. Phys. Chem.* **71,** 712 (1967).
8. Aniansson, G., Creaser, R. P., Held, W. D., Holmlid, L., and Toennies, J. P., *J. Chem. Phys.* **61,** 5381 (1974).
9. Holmlid, L., and Olsson, J. O., *Surface Sci.* **55,** 523 (1976).
10. Holmlid, L., and Olsson, J. O., *Surface Sci.* **67,** 61 (1977).
11. Miller, W. B., Safron, S. A., and Herschbach, D. R., *Discuss. Faraday Soc.* **44,** 108 and 292 (1967).
12. Holmlid, L., and Olsson, J. O., to be published.
13. Pasternak, L., and Dagdigian, P. J., *Rev. Sci. Instrum.* **48,** 226 (1977).
14. Rekova, L. P., Mozgin, V. V., Zvyagintseva, L. N., Bondarenko, V. N., and Fogel, Ya.M., *Sov. Phys. Tech. Phys.* **10,** 1465 (1975).
15. Palmberg, P. W., *in* "The Structure and Chemistry of Solid Surfaces" (G. A. Somorjai, Ed.). Wiley, New York, 1969.
16. Wilf, W., and Dawson, P. T., *Surface Sci.* **65,** 399 (1977).
17. Touw, T. R., and Trischka, J. W., *J. Appl. Phys.* **34,** 3635 (1963).
18. Holmlid, L., and Sundby, E., unpublished.
19. Holmlid, L., and Olsson, J. O. Paper 4 in Dissertation (J. O. Olsson), University of Göteborg, 1977.
20. Gerlach, R. L., and Rhodin, T. N., *Surface Sci.* **19,** 403 (1970).
21. Olsson, J. O., and Holmlid, L., *Mater. Sci. Eng.* **42,** 121 (1980).
22. Scheer, M. D., Klein, R., and McKinley, J. D., *J. Chem. Phys.* **55,** 3577 (1971).
23. Armand, G., *Surface Sci.* **66,** 321 (1977).
24. Matsumoto, S., Tomoda, S., and Kusunoki, I., *Bull. Res. Inst. Sci. Meas. Tohoku Univ. (Japan)* **23,** 91 (1974).
25. Roach, A. C., and Child, M. S., *Mol. Phys.* **14,** 1 (1968).
26. Bauer, S. H., and Porter, R. F., *in* "Molten Salt Chemistry" (M. Blander, Ed.). Interscience, New York, 1964.
27. Welch, D. O., Lazareth, O. W., Dienes, G. J., and Hatcher, R. D., *J. Chem. Phys.* **64,** 835 (1976).
28. Zandberg, É. Ya., Tontegode, A. Ya., and Yusifov, F. K., *Sov. Phys. Tech. Phys.* **17,** 134 (1972).
29. Zandberg, É. Ya., and Paleev, V. I., *Sov. Phys. Tech. Phys.* **9,** 1575 (1965).
30. Potekhina, N. D., *Sov. Phys. Tech. Phys.* **15,** 479 (1970).